Mutations in *RAB28*, Encoding a Farnesylated Small GTPase, Are Associated with Autosomal-Recessive Cone-Rod Dystrophy

Susanne Roosing,[1,2,3] Klaus Rohrschneider,[4] Avigail Beryozkin,[5] Dror Sharon,[5] Nicole Weisschuh,[6] Jennifer Staller,[6] Susanne Kohl,[6] Lina Zelinger,[5] Theo A. Peters,[2,7,8] Kornelia Neveling,[1,3] Tim M. Strom,[9,10] European Retinal Disease Consortium, L. Ingeborgh van den Born,[11] Carel B. Hoyng,[12] Caroline C.W. Klaver,[13,14] Ronald Roepman,[1,2,3] Bernd Wissinger,[6,15] Eyal Banin,[5,15] Frans P.M. Cremers,[1,2,15] and Anneke I. den Hollander[1,2,3,12,15,*]

The majority of the genetic causes of autosomal-recessive (ar) cone-rod dystrophy (CRD) are currently unknown. A combined approach of homozygosity mapping and exome sequencing revealed a homozygous nonsense mutation (c.565C>T [p.Glu189*]) in *RAB28* in a German family with three siblings with arCRD. Another homozygous nonsense mutation (c.409C>T [p.Arg137*]) was identified in a family of Moroccan Jewish descent with two siblings affected by arCRD. All five affected individuals presented with hyperpigmentation in the macula, progressive loss of the visual acuity, atrophy of the retinal pigment epithelium, and severely reduced cone and rod responses on the electroretinogram. *RAB28* encodes a member of the Rab subfamily of the RAS-related small GTPases. Alternative RNA splicing yields three predicted protein isoforms with alternative C-termini, which are all truncated by the nonsense mutations identified in the arCRD families in this report. Opposed to other Rab GTPases that are generally geranylgeranylated, RAB28 is predicted to be farnesylated. Staining of rat retina showed localization of RAB28 to the basal body and the ciliary rootlet of the photoreceptors. Analogous to the function of other RAB family members, RAB28 might be involved in ciliary transport in photoreceptor cells. This study reveals a crucial role for RAB28 in photoreceptor function and suggests that mutations in other Rab proteins may also be associated with retinal dystrophies.

Cone-rod dystrophy (CRD [MIM 120970]) is characterized by primary loss of cone photoreceptors and subsequent or simultaneous loss of rod photoreceptors. The symptoms include poor visual acuity, disturbances in color vision, decreased sensitivity of the central visual field, and photo aversion. Because rods are also involved, impairment of night vision and peripheral vision loss can occur. The fundus appearance can vary from normal to a bull's eye maculopathy, or to marked atrophy of the macular region, with a variable degree of temporal pallor of the optic disc.[1] Visual fields display a central scotoma and full-field electroretinography (ERG) records a progressive deterioration of cone-derived amplitude responses, which are more reduced than, or equally reduced as, rod-derived responses.

CRD has an estimated prevalence of 1:30,000 to 1:40,000[1–3] and displays all types of Mendelian inheritance. Seven genes have been implicated in the autosomal recessive (ar) form, the most prevalent mode of inheritance, i.e., *ABCA4* (MIM 601691),[4] *ADAM9* (MIM 602713),[5] *C8orf37* (MIM 614477),[6] *CERKL* (MIM 608381),[7] *EYS* (MIM 612424),[8,9] *RPGRIP1* (MIM 605446),[10] and *TULP1* (MIM 602280).[11] However, mutations in these genes explain only a minority of the cases.[12]

The goal in this study was to identify genes underlying arCRD by using a combined approach of homozygosity mapping and exome sequencing. Such an approach has proven to be very effective in the discovery of genetic defects in several rare autosomal recessive diseases.[13–16] This study was approved by the local medical ethics committees and adhered to the tenets of the Declaration of Helsinki. All participants provided written informed consent prior to participation in the study.

To localize the genetic defect in a German family with three siblings affected by CRD (family A; Figure 1), the DNA of all three affected individuals was analyzed by using Affymetrix GeneChip Human Mapping 250K SNP arrays (Affymetrix, Santa Clara, CA, USA), and regions of homozygosity were calculated with Partek Genomics Suite software (Partek, St. Louis, MO, USA). This analysis revealed

[1]Department of Human Genetics, Radboud University Medical Centre, 6500 HB Nijmegen, the Netherlands; [2]Nijmegen Centre for Molecular Life Sciences, Radboud University Medical Centre, 6500 HB Nijmegen, the Netherlands; [3]Institute for Genetic and Metabolic Disease, Radboud University Medical Centre, 6500 HB Nijmegen, the Netherlands; [4]Department of Ophthalmology, University of Heidelberg, 69120 Heidelberg, Germany; [5]Departments of Ophthalmology, Hadassah-Hebrew University Medical Center, Jerusalem 91120, Israel; [6]Molecular Genetics Laboratory, Institute for Ophthalmic Research, Centre for Ophthalmology, University of Tuebingen, 72076 Tuebingen, Germany; [7]Department of Otorhinolaryngology, Radboud University Medical Centre, 6500 HB Nijmegen, the Netherlands; [8]Donders Institute for Brain, Cognition and Behaviour, Radboud University Medical Centre, 6500 HB Nijmegen, the Netherlands; [9]Institute of Human Genetics, Technische Universität München, 81675 Munich, Germany; [10]Institute of Human Genetics, Helmholtz Zentrum München, Neuherberg, 85764 Neuherberg, Germany; [11]The Rotterdam Eye Hospital, 3000 LM Rotterdam, the Netherlands; [12]Department of Ophthalmology, Radboud University Medical Centre, 6500 HB Nijmegen, the Netherlands; [13]Department of Ophthalmology, Erasmus Medical Centre, 3000 CA Rotterdam, the Netherlands; [14]Epidemiology, Erasmus Medical Centre, 3000 CA Rotterdam, the Netherlands
[15]These authors contributed equally to this work
*Correspondence: a.denhollander@ohk.umcn.nl
http://dx.doi.org/10.1016/j.ajhg.2013.05.005.

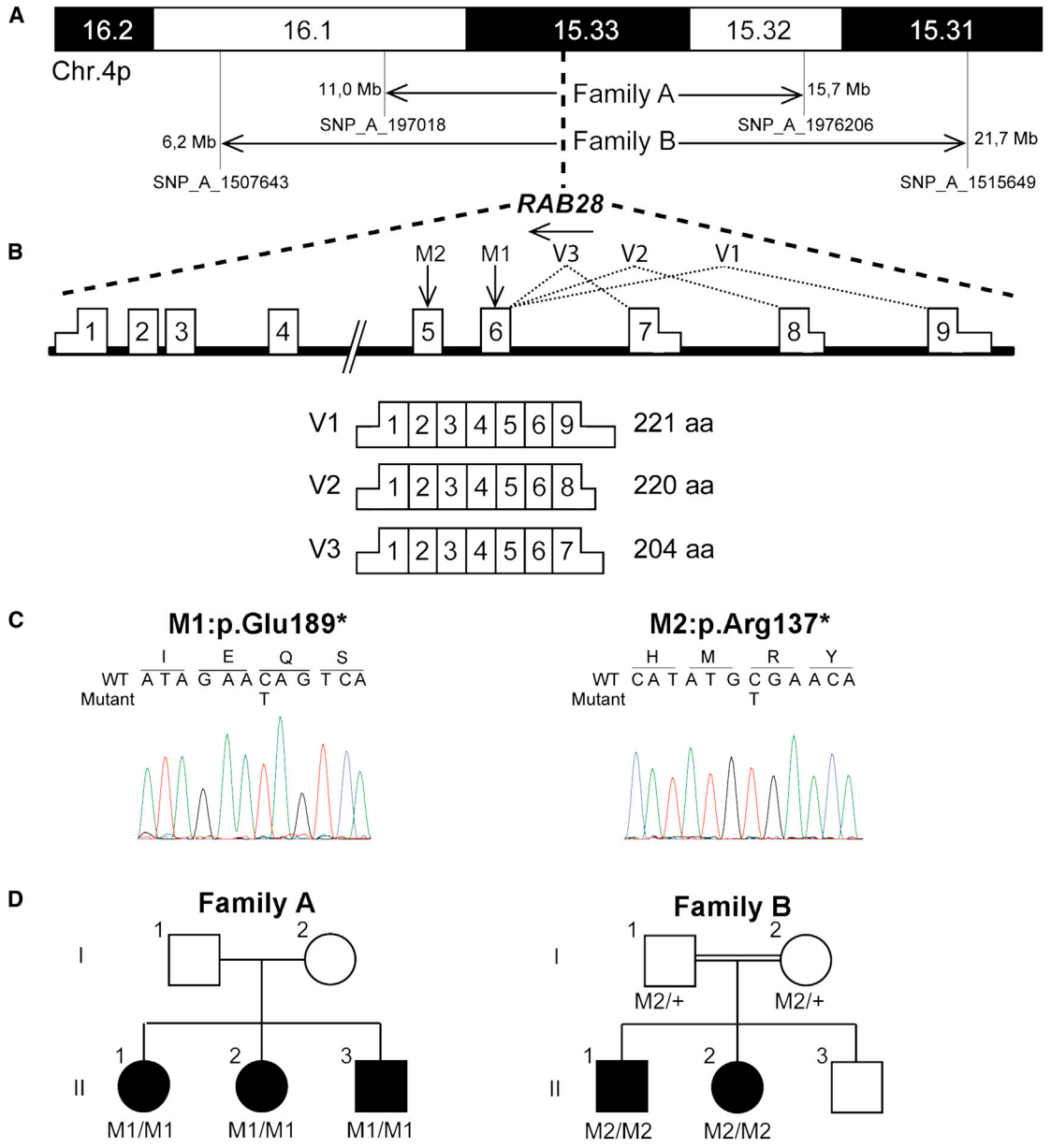

Figure 1. Chromosome 4 Homozygous Regions and *RAB28* Mutations in Two Families with arCRD

(A) Shown are chromosomal position of *RAB28* and location of the homozygous regions identified in families A and B by using homozygosity mapping.

(B) Genomic structure and mRNA variants of *RAB28*. Variant 1 (V1) encodes a 221 amino acid (aa) protein isoform (RAB28S [NM_001017979.2]), variant 2 (V2) encodes a 220 aa protein isoform (RAB28L [NM_004249.3]), and variant 3 (V3) encodes a predicted 204 aa protein (HST03798 [NM_001159601.1]). The location of the nonsense mutations found in families A (mutation M1) and B (mutation M2) are indicated.

(C) Sanger sequencing confirmed the segregation of the homozygous nonsense mutations M1 (c.565C>T [p.Glu189*]) in family A and M2 (c.409C>T [p.Arg137*]) in family B.

(D) Pedigrees of family A of German ancestry and family B of Moroccan Jewish ancestry, demonstrating the segregation of the nonsense mutations in *RAB28*.

a shared homozygous region of 4.68 Mb on chromosome 4 in all three affected siblings (see Table S1 available online) containing 15 genes. Subsequently, exome sequencing was performed in two out of three affected siblings (A-II:1 and A-II:2). Exome sequencing was performed on a SOLiD4 sequencing platform (Life Technologies, Carlsbad, CA, USA), and the exomes were enriched according to the manufacturer's protocol by using Agilent's SureSelect Human All Exon v.2 Kit (50 Mb), containing the exonic sequences of approximately 21,000 genes (Agilent Technologies, Inc., Santa Clara, CA, USA). LifeScope software v2.1 (Life Technologies, Carlsbad, CA, USA) was used to map color space reads along the hg19 reference genome assembly. The DiBayes algorithm, with high-stringency calling, was used for single-nucleotide variant calling. The small Indel Tool was used to detect small insertions and

deletions. For the analyzed individuals, a total of 83,287,089 and 76,841,552 reads were uniquely mapped to the gene-coding regions, respectively, with a median coverage of 67.3× in person A-II:1 and 61.9× in person A-II:2. The analysis uncovered 39,561 variants for individual A-II:1 and 39,029 variants for individual A-II:2. Ninety-six nonsynonymous exonic and canonical splice-site variants, occurring with a frequency of less than 1% in 1,154 unrelated individuals (in-house exome database), were shared by both individuals (data not shown). No pathogenic variants in the genes known to be mutated in arCRD (*ABCA4*, *ADAM9*, *C8orf37*, *CERKL*, *EYS*, *RPGRIP1*, and *TULP1*) were observed among the shared variants. Under the hypothesis of autosomal recessive inheritance, we did not identify two heterozygous variants in a single gene (>20%–<80% variation) in both affected individuals and only a single homozygous (>80% variation) variant, p.Glu189*(c.565C>T [NM_001017979.2]), in *RAB28* (MIM 612994). This variant is located in the largest shared homozygous region in family A (Figure 1A; Table S1).

Sanger sequencing confirmed the homozygous presence of c.565C>T in the three affected siblings (Figures 1C and 1D). The mutation was not identified in 176 ethnically matched controls or in the Exome Variant Server (EVS) database (release ESP6500).

Primers to amplify all coding exons and their exon-intron boundaries were designed by using Primer 3 software (Table S2). Sanger sequencing of all coding exons of *RAB28* in 468 unrelated CRD and 149 unrelated individuals with cone dystrophy did not identify additional likely pathogenic mutations. We assessed SNP data of >400 unrelated individuals with arCRD, Leber congenital amaurosis (LCA), and retinitis pigmentosa (RP) through the European Retinal Disease Consortium[6,17] and identified seven families with conspicuously large homozygous regions spanning *RAB28*. Sanger sequencing of *RAB28* in these families revealed a homozygous nonsense mutation (c.409C>T [p.Arg137*]) in a consanguineous family (family B) of Moroccan Jewish ancestry. The two affected siblings in family B (II:1 and II:2; Figure 1) shared four homozygous genomic regions (over 10 Mb) by whole-genome SNP analysis (Table S1). The largest region was on chromosome 7 and the second largest region was on chromosome 4, the latter including 315 genes among which *OPN1SW* (MIM 613522), and *RAB28*. Mutation analysis of *OPN1SW* did not yield causative variants. Segregation analysis confirmed the presence of the homozygous nonsense mutation in *RAB28* in both siblings with CRD (Figures 1C and 1D). This mutation was not identified in 118 ethnically matched controls or in the EVS database.

The clinical features of the affected individuals of both families are described in Table 1. Members of family A were diagnosed with CRD in the second decade of life, with rapidly deteriorating visual acuities and high myopia. At their last visit, fundoscopy showed hyperpigmention of the fovea and autofluorescence revealed a slight hyperfluorescent fovea (Figures 2A and 2B). Optical coherence tomography (OCT) displayed altered photoreceptors in the fovea, whereas the peripheral photoreceptors are intact (Figure 2C). Color-vision tests revealed defects in all axes, and visual field testing showed a central scotoma. On ERG photopic responses were nondetectable and scotopic responses reduced in all three siblings. The clinical presentation of both affected individuals of family B was comparable to that of family A. Individual B-II:1 presented with low vision since early childhood, with progressive deterioration of the visual acuity and high myopia. The retinal pigment epithelium showed foveal atrophy, hypofluorescence was observed in the fovea, and a hyperfluorescent ring was noted around the fovea (Figures 2D and 2E, respectively). OCT imaging confirmed absence of photoreceptors in the central fovea, whereas the photoreceptor layer further out appears largely intact (Figure 2F). Color-vision defects were noted in both siblings. Photopic ERG responses were nondetectable, and scotopic responses were moderately reduced.

RAB28 encodes a member of the Rab ("Ras-related in brain")[18] subfamily of the RAS-related small GTPases. Rab GTPases are key regulators in trafficking of proteins and function as molecular switches to regulate fusion steps in vesicle transport, vesicle budding, motility, tethering,[19] and membrane fission.[20] Proper membrane association and subcellular localization of Rab proteins requires post-translational prenylation of cysteine motif(s) at the carboxyl terminus, which for the majority of Rabs involves the attachment of a geranylgeranyl (20 carbons) anchor by geranylgeranyltransferase II (GGT2 or RabGGT). RAB28 is a rather distant relative of the at least 60 different Rabs,[21] standing out because of its limited similarity (32% amino acid identity) to other Rab GTPases and its specific amino acid motifs.[21–23] RAB28 expresses three mRNA variants encoding different RAB28 isoforms with alternative C-termini (see Figure 1B).[22] Another unique feature of RAB28 is that isoforms 1 and 2 are predicted to be farnesylated at their CaaX-motifs,[22–25] which was experimentally proven for isoform 1 of RAB28.[25] The third isoform does not contain a CaaX-motif and therefore cannot be prenylated.

Wide expression is found for variant 1 in contrast to variant 2, which has been reported to be primarily expressed in testis.[22] Expression analysis in RNA samples from various human tissues showed highest expression of variant 1 in lung, bone marrow, retinal pigment epithelium (RPE), and kidney, wide and abundant expression of variant 2, and highest expression of variant 3 in heart, lung, bone marrow, retina, brain and RPE (Figure S1). Staining of rat retina showed localization of RAB28 to the basal body and the ciliary rootlet of the photoreceptors (Figure 3; Figure S3).

Both nonsense mutations identified in the CRD families in this report are found in the shared mRNA segment, and are therefore predicted to truncate all three RAB28 isoforms. To determine whether the *RAB28* mRNA is subjected to nonsense-mediated decay (NMD), RT-PCR

Table 1. Summary of the Clinical Data of Five Individuals with *RAB28* Mutations

Individual	Ancestry	Diagnosis	Age at Diagnosis	Age at Last Visit	Refractive Error at Last Visit	Visual Acuity at Last Visit	Fundus	Autofluorescence	OCT	Color Vision	Visual Field (Goldmann)	ERG
Family A												
A-II:1	German	CRD	14 years	28	OD −16D SE OS −15.5D SE	OD 20/320 OS 20/200	Hyperpigmented foveal region	Hyperfluorescent area at foveal region	Irregular inner and outer segments in fovea, thinning of other retinal layers of fovea	D-15 Panel: tritan and defects in scotopic lines	Concentric reduction to 15–20 degrees (III/4)	Age 16: nondetectable cone function and reduced rod responses
A-II:2	German	CRD	12 years	25	OD −19D SE OS −22D SE	OD 20/320 OS 20/50	Hyperpigmented foveal region	Hyperfluorescent area at foveal region	Irregular inner and outer segments in fovea, thinning of other retinal layers of fovea	D-15 Panel saturated: tritan defects, desaturated: marked protan defects	Concentric reduction to 30–40 degrees (III/4)	Age 13: nondetectable photopic and markedly reduced scotopic ERG
A-II:3	German	CRD	10 years	16	OD −6.5D SE OS −7.0D SE	OD 20/80 OS 20/60	Hyperpigmented foveal region	NA	NA	Diffuse errors	Central scotoma	Age 10: nondetectable cone responses under photopic conditions, rod responses under scotopic conditions slightly reduced; age 15: scotopic markedly reduced
Family B												
B-II:1	Moroccan Jewish	CRD	Early childhood	33	OU −11D SE	OU 20/125	Atrophy (geographic atrophy-like) in fovea. White without pressure in periphery. Tilted optic discs (OS > OD) with temporal pallor OS.	Ring of hyperfluorescence	Atrophy in fovea; retinal layers absent at foveal region	D-15 Panel: OD scotopic lines; OS Tritan and Deutan defect	NA	Age 30: nondetectable cone responses under photopic response; rod responses under scotopic responses moderately reduced (30% below normal). Mixed cone-rod response moderately to severely reduced (?50%–60% below normal)
B-II:2	Moroccan Jewish	CD/CRD	NA	30	NA	NA				D-15 Panel: Deutan defect and scotopic lines, more severe in OS	NA	Age 30: nondetectable cone responses under photopic condition; rod responses under scotopic response at below normal in OD and within normal limits in OS. Mixed cone-rod response moderately reduced (?25%–35% below normal)

D, diopters; ERG, electroretinogram; OCT, optical coherence tomography; OD, right eye; OS, left eye; OU, both eyes; RPE, retinal pigment epithelium; SE, spherical equivalent.

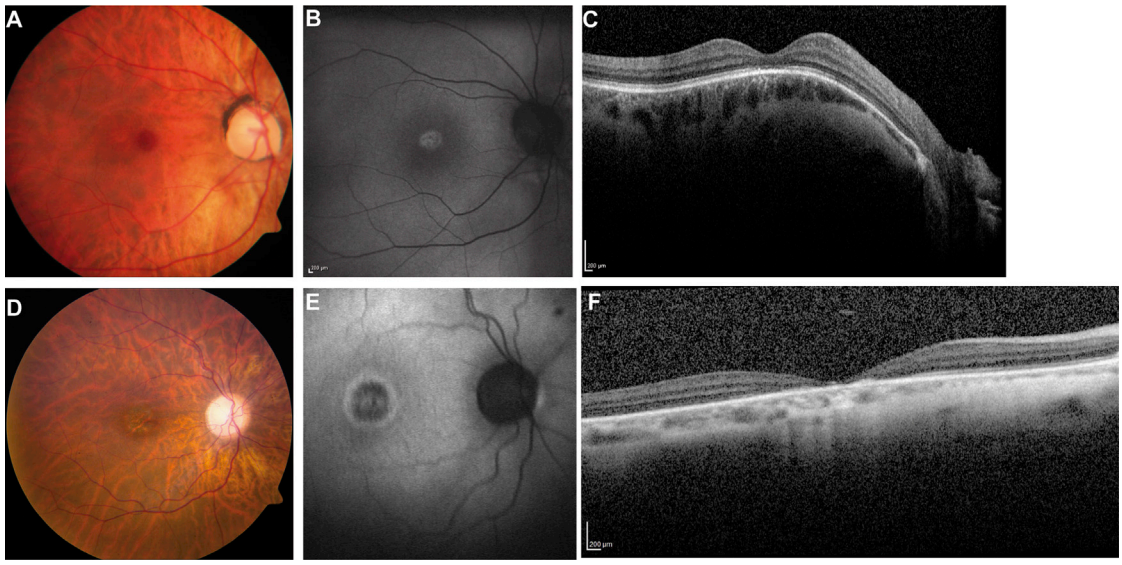

Figure 2. Clinical Presentation of CRD Associated with *RAB28* Mutations
(A–C) Retinal imaging of the right eye of individual A-II:2 of family A at age 25. (A) Fundus photography showed slight hyperpigmentation of the foveal region; (B) Autofluorescence imaging revealed a slight hyperfluorescent leash at the fovea without striking pathology (central brightening is an artifact); (C) Optical coherence tomography (OCT) displayed altered photoreceptors in the central fovea with an intact periphery.
(D–F) Retinal imaging of the right eye of individual B-II:1 of family B at age 33: (D) Fundus photographs showed foveal atrophy with no marked peripheral changes (E). Autofluorescence imaging revealed a hyperfluorescent ring surrounding the hypofluorescent fovea; (F) OCT scans confirm the presence of foveal atrophy while the photoreceptor layer is largely intact further out.

analysis was performed in RNA samples isolated from lymphocytes of affected individuals of families A and B by using a primer set amplifying exons 2 and 3, a region that is shared by all three RAB28 isoforms, and three different primer sets to evaluate the expression of the three isoforms individually. *RAB28* transcript was detected in affected members of both families, excluding complete loss of *RAB28* transcript by NMD (Figure S2).

The exact role of RAB28 in cone and rod photoreceptors remains to be determined. The localization of RAB28 to the basal body and ciliary rootlet suggests a role in ciliary transport. Interestingly, RAB8 and RAB11, which have so far not been shown to be associated with disease, coordinate primary ciliogenesis[28] and together with RAB3A and RAB6A are involved in rhodopsin transport from the photoreceptor inner to outer segments through the connecting cilium.[29–32] RAB28 may have adopted a similar function with specific importance for the highly active vesicle-based transport of photoreceptor proteins through the connecting cilium. Identification of *RAB28* mutations emphasizes the role of disrupted ciliary processes in the pathogenesis of CRD. In addition to RAB28, three proteins involved in CRD (C8orf37, RPGRIP1, and TULP1) have so far been shown to localize to the connecting cilia of photoreceptor cells, and approximately one third of the gene defects underlying retinal degeneration affect the connecting cilium structure and/or function in photoreceptors.[33] The observation that nonsense mutations in *RAB28* cause a phenotype only in the eye may point to functional redundancy in other tissues.

In conclusion, a combined approach of homozygosity mapping and exome sequencing identified nonsense mutations in *RAB28* as a rare cause of arCRD. This study reveals a crucial role for RAB28 in photoreceptor function and suggests that mutations in other Rab proteins may also be associated with retinal dystrophies. The functional implications of *RAB28* mutations remain unclear and warrant further investigation.

Supplemental Data

Supplemental Data includes three figures and three tables and can be found with this article online at http://www.cell.com/AJHG.

Acknowledgments

We thank the individuals and their families for participating in this study. We thank Riet Bernaerts-Biskop, Rob W.J. Collin, Christian F.H.A. Gilissen, Arjen Henkes, Michael P. Kwint, Hans Scheffer, Marloes Steehouwer, Saskia D. van der Velde-Visser, Joris A. Veltman, Nienke A.W. Wieskamp, and Marijke Zonneveld for their valuable advice or expert assistance. We are thankful to Jose S. Ramalho for providing the pEGFP-RAB28 construct. We thank other members of the European Retinal Disease Consortium (Elfride De Baere, Tamar Ben-Yosef, Alejandro Garanto, Robert K. Koenekoop, Bart P. Leroy, Alberta A.H.J. Thiadens) for providing valuable samples and expertise. This study was financially supported by the Foundation Fighting Blindness USA (grants BR-GE-0510-04890RAD, C-GE-0811-0545-RAD01, and BR-GE-0510-0490-HUJ) to A.I.d.H, F.P.M.C., and D.S., the Algemene

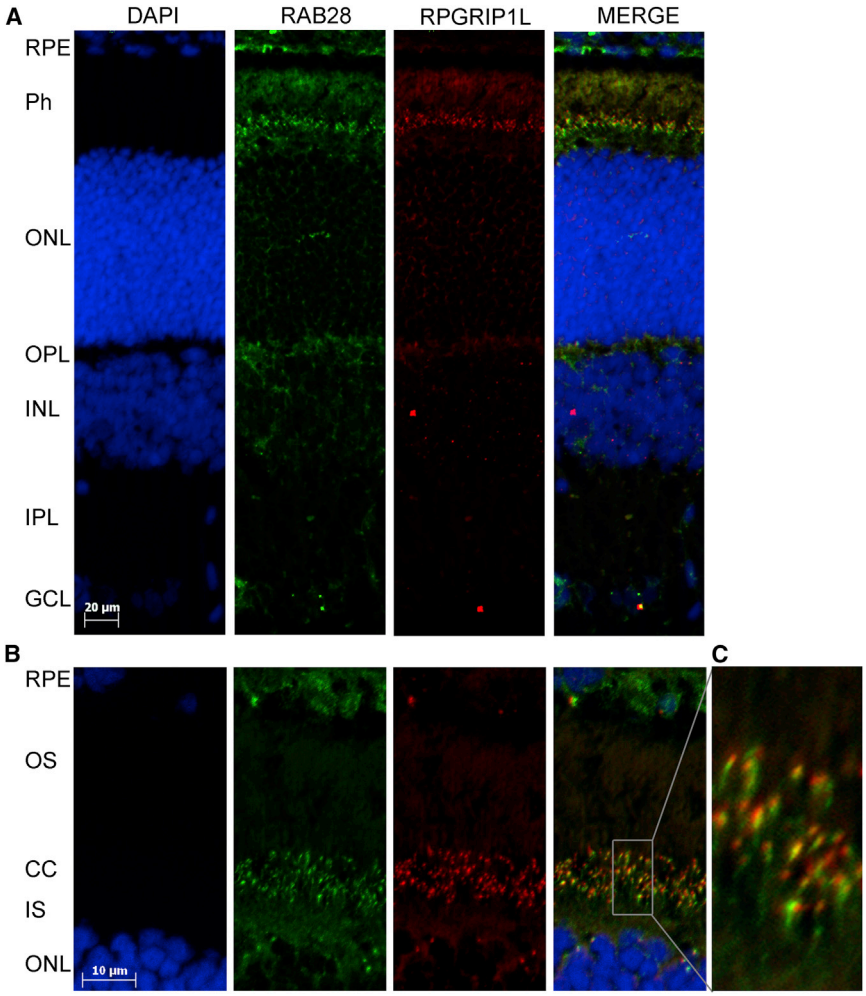

Figure 3. Subcellular Localization of RAB28 in Rat Retina

Cryosections of rat photoreceptor cells from day P20 were assessed by immunohistochemistry with mouse polyclonal α-RAB28 antibodies raised against aa 1–96 of human RAB28. These antibodies recognize all RAB28 isoforms (Sigma-Aldrich, SAB1406812, validated as shown in Figure S3). Affinity purified guinea pig-α-RPGRIP1L (SNC040) was used as a marker of the basal body of the connecting cilium, as shown previously.[26,27]

(A) Rat retinal sections from P20 were stained with DAPI (blue, first panel), α-RAB28 (green, second panel), and α-RPGRIP1L (red, third panel). The merged image in the right panel shows the colocalization of RAB28 and RPGRIP1L.

(B) Enlargement of the photoreceptor layer, demonstrating partial colocalization of RAB28 and RPGRIP1L at the base of the connecting cilium.

(C) A higher magnification of the connecting cilium region. The retinal layers are retinal pigment epithelium (RPE), photoreceptor layer (Ph), outer nuclear layer (ONL), outer plexiform layer (OPL), outer segment (OS), connecting cilium (CC), inner segment (IS), inner plexiform layer (IPL), and ganglion cell layer (GCL).

Nederlandse Vereniging ter Voorkoming van Blindheid, the Gelderse Blinden Stichting, the Landelijke Stichting voor Blinden en Slechtzienden, the Stichting Blinden-Penning, the Stichting Macula Degeneratie fonds, and the Rotterdamse Stichting Blindenbelangen (to F.P.M.C. and C.C.W.K.), by the Yedidut Research Grant (to E.B.), a Netherlands Organization for Scientific Research (NWO Vidi-91786396 and Vici-016.130.664 to R.R.), and a BMBF grant (01GM1108A) to B.W. and S.K.. The work was supported by the German Ministry of Education and Research (01GR0802 and 01GM0867) and the European Commission 7th Framework Program (261123, GEUVADIS) to T.M.S.

Received: October 19, 2012
Revised: March 27, 2013
Accepted: May 3, 2013
Published: June 6, 2013

Web Resources

The URLs for data presented herein are as follows:

Exome Variant Server (EVS) database, release ESP6500, http://evs.gs.washington.edu/EVS/

Online Mendelian Inheritance in Man (OMIM), http://www.omim.org/

Primer3, http://frodo.wi.mit.edu/primer3/

References

1. Hamel, C.P. (2007). Cone rod dystrophies. Orphanet J. Rare Dis. *2*, 7.
2. Michaelides, M., Hunt, D.M., and Moore, A.T. (2004). The cone dysfunction syndromes. Br. J. Ophthalmol. *88*, 291–297.
3. Thiadens, A.A.H.J., den Hollander, A.I., Roosing, S., Nabuurs, S.B., Zekveld-Vroon, R.C., Collin, R.W.J., De Baere, E., Koenekoop, R.K., van Schooneveld, M.J., Strom, T.M., et al. (2009). Homozygosity mapping reveals PDE6C mutations in patients with early-onset cone photoreceptor disorders. Am. J. Hum. Genet. *85*, 240–247.
4. Cremers, F.P.M., van de Pol, D.J., van Driel, M., den Hollander, A.I., van Haren, F.J., Knoers, N.V., Tijmes, N., Bergen, A.A., Rohrschneider, K., Blankenagel, A., et al. (1998). Autosomal recessive retinitis pigmentosa and cone-rod dystrophy caused by splice site mutations in the Stargardt's disease gene ABCR. Hum. Mol. Genet. *7*, 355–362.
5. Parry, D.A., Toomes, C., Bida, L., Danciger, M., Towns, K.V., McKibbin, M., Jacobson, S.G., Logan, C.V., Ali, M., Bond, J., et al. (2009). Loss of the metalloprotease ADAM9 leads to cone-rod dystrophy in humans and retinal degeneration in mice. Am. J. Hum. Genet. *84*, 683–691.
6. Estrada-Cuzcano, A.I., Neveling, K., Kohl, S., Banin, E., Rotenstreich, Y., Sharon, D., Falik-Zaccai, T.C., Hipp, S., Roepman,

R., Wissinger, B., et al.; European Retinal Disease Consortium. (2012). Mutations in C8orf37, encoding a ciliary protein, are associated with autosomal-recessive retinal dystrophies with early macular involvement. Am. J. Hum. Genet. *90*, 102–109.
7. Tuson, M., Marfany, G., and Gonzàlez-Duarte, R. (2004). Mutation of CERKL, a novel human ceramide kinase gene, causes autosomal recessive retinitis pigmentosa (RP26). Am. J. Hum. Genet. *74*, 128–138.
8. Collin, R.W.J., Littink, K.W., Klevering, B.J., van den Born, L.I., Koenekoop, R.K., Zonneveld, M.N., Blokland, E.A., Strom, T.M., Hoyng, C.B., den Hollander, A.I., and Cremers, F.P.M. (2008). Identification of a 2 Mb human ortholog of Drosophila eyes shut/spacemaker that is mutated in patients with retinitis pigmentosa. Am. J. Hum. Genet. *83*, 594–603.
9. Abd El-Aziz, M.M., Barragan, I., O'Driscoll, C.A., Goodstadt, L., Prigmore, E., Borrego, S., Mena, M., Pieras, J.I., El-Ashry, M.F., Safieh, L.A., et al. (2008). EYS, encoding an ortholog of Drosophila spacemaker, is mutated in autosomal recessive retinitis pigmentosa. Nat. Genet. *40*, 1285–1287.
10. Hameed, A., Abid, A., Aziz, A., Ismail, M., Mehdi, S.Q., and Khaliq, S. (2003). Evidence of RPGRIP1 gene mutations associated with recessive cone-rod dystrophy. J. Med. Genet. *40*, 616–619.
11. Roosing, S., van den Born, L.I., Hoyng, C.B., Thiadens, A.A.H.J., de Baere, E., Collin, R.W., Koenekoop, R.K., Leroy, B.P., van Moll-Ramirez, N., Venselaar, H., et al. (2013). Maternal uniparental isodisomy of chromosome 6 reveals a TULP1 mutation as a novel cause of cone dysfunction. Ophthalmology. Published online March 14, 2013. http://dx.doi.org/10.1016/j.ophtha.2012.12.005.
12. Littink, K.W., Koenekoop, R.K., van den Born, L.I., Collin, R.W.J., Moruz, L., Veltman, J.A., Roosing, S., Zonneveld, M.N., Omar, A., Darvish, M., et al. (2010). Homozygosity mapping in patients with cone-rod dystrophy: novel mutations and clinical characterizations. Invest. Ophthalmol. Vis. Sci. *51*, 5943–5951.
13. Zangen, D., Kaufman, Y., Zeligson, S., Perlberg, S., Fridman, H., Kanaan, M., Abdulhadi-Atwan, M., Abu Libdeh, A., Gussow, A., Kisslov, I., et al. (2011). XX ovarian dysgenesis is caused by a PSMC3IP/HOP2 mutation that abolishes coactivation of estrogen-driven transcription. Am. J. Hum. Genet. *89*, 572–579.
14. Walsh, T., Shahin, H., Elkan-Miller, T., Lee, M.K., Thornton, A.M., Roeb, W., Abu Rayyan, A., Loulus, S., Avraham, K.B., King, M.C., and Kanaan, M. (2010). Whole exome sequencing and homozygosity mapping identify mutation in the cell polarity protein GPSM2 as the cause of nonsyndromic hearing loss DFNB82. Am. J. Hum. Genet. *87*, 90–94.
15. Sirmaci, A., Walsh, T., Akay, H., Spiliopoulos, M., Sakalar, Y.B., Hasanefendioğlu-Bayrak, A., Duman, D., Farooq, A., King, M.C., and Tekin, M. (2010). MASP1 mutations in patients with facial, umbilical, coccygeal, and auditory findings of Carnevale, Malpuech, OSA, and Michels syndromes. Am. J. Hum. Genet. *87*, 679–686.
16. Gilissen, C., Arts, H.H., Hoischen, A., Spruijt, L., Mans, D.A., Arts, P., van Lier, B., Steehouwer, M., van Reeuwijk, J., Kant, S.G., et al. (2010). Exome sequencing identifies WDR35 variants involved in Sensenbrenner syndrome. Am. J. Hum. Genet. *87*, 418–423.
17. Ozgül, R.K., Siemiatkowska, A.M., Yücel, D., Myers, C.A., Collin, R.W.J., Zonneveld, M.N., Beryozkin, A., Banin, E., Hoyng, C.B., van den Born, L.I., et al.; European Retinal Disease Consortium. (2011). Exome sequencing and cis-regulatory mapping identify mutations in MAK, a gene encoding a regulator of ciliary length, as a cause of retinitis pigmentosa. Am. J. Hum. Genet. *89*, 253–264.
18. Touchot, N., Chardin, P., and Tavitian, A. (1987). Four additional members of the ras gene superfamily isolated by an oligonucleotide strategy: molecular cloning of YPT-related cDNAs from a rat brain library. Proc. Natl. Acad. Sci. USA *84*, 8210–8214.
19. Stenmark, H., and Olkkonen, V.M. (2001). The Rab GTPase family. Genome Biol *2*, S3007.
20. Miserey-Lenkei, S., Chalancon, G., Bardin, S., Formstecher, E., Goud, B., and Echard, A. (2010). Rab and actomyosin-dependent fission of transport vesicles at the Golgi complex. Nat. Cell Biol. *12*, 645–654.
21. Pereira-Leal, J.B., and Seabra, M.C. (2001). Evolution of the Rab family of small GTP-binding proteins. J. Mol. Biol. *313*, 889–901.
22. Brauers, A., Schürmann, A., Massmann, S., Mühl-Zürbes, P., Becker, W., Kainulainen, H., Lie, C., and Joost, H.G. (1996). Alternative mRNA splicing of the novel GTPase Rab28 generates isoforms with different C-termini. Eur. J. Biochem. *237*, 833–840.
23. Lee, S.H., Baek, K., and Dominguez, R. (2008). Large nucleotide-dependent conformational change in Rab28. FEBS Lett. *582*, 4107–4111.
24. Maurer-Stroh, S., and Eisenhaber, F. (2005). Refinement and prediction of protein prenylation motifs. Genome Biol. *6*, R55.
25. Maurer-Stroh, S., Koranda, M., Benetka, W., Schneider, G., Sirota, F.L., and Eisenhaber, F. (2007). Towards complete sets of farnesylated and geranylgeranylated proteins. PLoS Comput. Biol. *3*, e66.
26. Arts, H.H., Doherty, D., van Beersum, S.E., Parisi, M.A., Letteboer, S.J., Gorden, N.T., Peters, T.A., Märker, T., Voesenek, K., Kartono, A., et al. (2007). Mutations in the gene encoding the basal body protein RPGRIP1L, a nephrocystin-4 interactor, cause Joubert syndrome. Nat. Genet. *39*, 882–888.
27. Coene, K.L.M., Mans, D.A., Boldt, K., Gloeckner, C.J., van Reeuwijk, J., Bolat, E., Roosing, S., Letteboer, S.J.F., Peters, T.A., Cremers, F.P.M., et al. (2011). The ciliopathy-associated protein homologs RPGRIP1 and RPGRIP1L are linked to cilium integrity through interaction with Nek4 serine/threonine kinase. Hum. Mol. Genet. *20*, 3592–3605.
28. Knödler, A., Feng, S., Zhang, J., Zhang, X., Das, A., Peränen, J., and Guo, W. (2010). Coordination of Rab8 and Rab11 in primary ciliogenesis. Proc. Natl. Acad. Sci. USA *107*, 6346–6351.
29. Deretic, D., Huber, L.A., Ransom, N., Mancini, M., Simons, K., and Papermaster, D.S. (1995). rab8 in retinal photoreceptors may participate in rhodopsin transport and in rod outer segment disk morphogenesis. J. Cell Sci. *108*, 215–224.
30. Satoh, A.K., O'Tousa, J.E., Ozaki, K., and Ready, D.F. (2005). Rab11 mediates post-Golgi trafficking of rhodopsin to the photosensitive apical membrane of Drosophila photoreceptors. Development *132*, 1487–1497.

31. Deretic, D. (1997). Rab proteins and post-Golgi trafficking of rhodopsin in photoreceptor cells. Electrophoresis *18*, 2537–2541.
32. Moritz, O.L., Tam, B.M., Hurd, L.L., Peränen, J., Deretic, D., and Papermaster, D.S. (2001). Mutant rab8 impairs docking and fusion of rhodopsin-bearing post-Golgi membranes and causes cell death of transgenic Xenopus rods. Mol. Biol. Cell *12*, 2341–2351.
33. Estrada-Cuzcano, A., Roepman, R., Cremers, F.P.M., den Hollander, A.I., and Mans, D.A. (2012). Non-syndromic retinal ciliopathies: translating gene discovery into therapy. Hum. Mol. Genet. *21*(R1), R111–R124.